



Influence of the moisture content on the fracture energy and tensile strength of hardwood spotted gum sawn timber and adhesive bonds (gluelines)

Peiqing Lu¹ · Benoit P. Gilbert^{1,2} · Chandan Kumar² · Robert L. McGavin^{1,2} · Hassan Karampour¹

Received: 25 March 2023 / Accepted: 24 August 2023 / Published online: 9 October 2023
© The Author(s) 2023

Abstract

This study aims to measure the fracture properties, including crack initiation and propagation, of Australia's native forest grown spotted gum ([SPG], *Corymbia citriodora*) sawn timber and associated adhesive bonds at different moisture content levels. The collected data were used as input values to develop a numerical model to understand the delamination of SPG glulam beams when exposed to a wetting and drying process. Thus, Mode I and Mode II fracture energies for crack propagation along radial and glueline directions were experimentally investigated under various moisture content levels (8%, 12% and 16%). Single-end notched beams and compact shear specimens were used to capture the Mode I and Mode II fracture energies, respectively. For crack initiation, the tensile strength perpendicular to the grain and the shear strength (taken as the maximum stress from the Mode II fracture tests) were also measured. In total, 200 experimental tests were performed. One-way analysis of variance statistical analyses showed that the fracture energies and shear strengths were independent of the range of moisture content levels investigated. In addition, the collected data were compared with the limited published fracture properties of other hardwood species.

1 Introduction

With the current drive towards sustainable and green construction, the demand for high-performance engineered wood products is increasing. This creates opportunities and challenges for Australia's hardwood industry, such as for native forest grown spotted gum ([SPG], *Corymbia citriodora*), a dense hardwood with superior mechanical properties and durability (Bootle 1983). SPG is an Australian native hardwood species that comprises about 70% of the annual hardwood logs supplied by Queensland (QLD) native forests (Queensland Government Department of Agriculture and Fisheries 2016). There is a drive to manufacture glulam from this species for use as beams, columns or bridge elements. However, for SPG glulam to be commercialised,

the bond between the boards must satisfy the delamination requirements of the Australian and New Zealand Standard AS/NZS 1328.1 (2011). The delamination test consists of vacuum water impregnation followed by a drying process. The parameters of these two processes depend on the service class of the final product (i.e., its intended environmental application). However, despite best efforts to improve the gluability of SPG (Leggate et al. 2022), SPG glulam products commonly do not meet the requirements of AS/NZS 1328.1 (2011) for external applications (see Fig. 1 for the outcomes of a typical delamination test). This phenomenon is thought to be attributed to (1) the difficulty in gluing the species as a result of the limited adhesive penetration (Leggate et al. 2021a) and (2) the high moisture shrinkage coefficients combined with the high elastic moduli of the material that cause large moisture-induced internal stresses to develop in the gluelines during the delamination test.

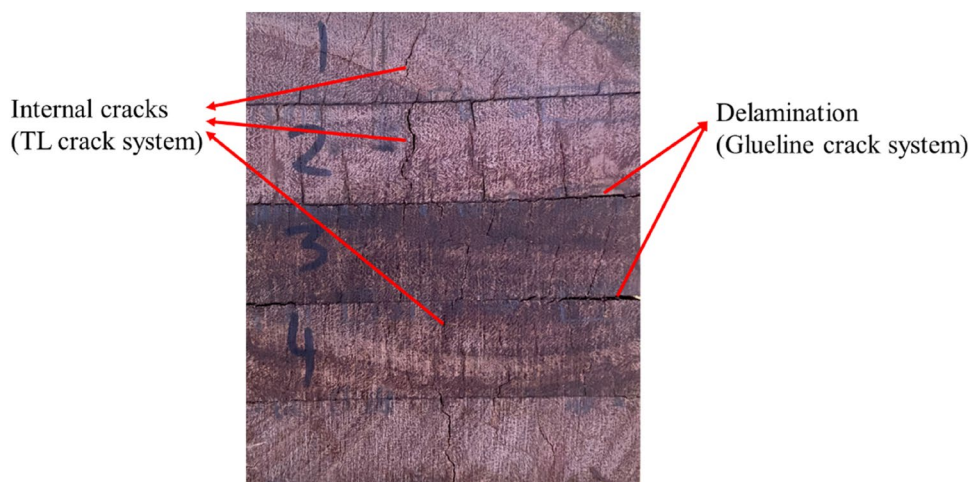
As delamination develops from over-stressed gluelines (Vella et al. 2019), mechanically reducing the internal stresses could represent an effective solution to prevent delamination. Several approaches could be adopted to prevent delamination. First, as the shrinkage and swelling coefficients of SPG (and timber in general) are different along the radial and tangential directions (Redman

✉ Peiqing Lu
peiqing.lu@griffithuni.edu.au

¹ School of Engineering and Built Environment, Griffith University, Gold Coast, QLD 4222, Australia

² Queensland Government Department of Agriculture and Fisheries, Forest Products Innovation, Salisbury Research Facility, Salisbury, QLD 4107, Australia

Fig. 1 Spotted gum glulam after delamination test



2017), designing the glulam with boards stacked in a specific grain orientation combination could improve the outcomes of the delamination test. Second, cutting stress relief grooves with specific shapes and arrangements in the boards could reduce the internal stresses (Raftery and Whelan 2014). Third, adjusting the board geometry (the width to thickness ratio) could affect the internal stresses and thus decrease the stresses imposed on the gluelines during the delamination test.

To test these three hypotheses, the development of a numerical model that can reproduce (i) the heat-and-mass transfer in the glulam during drying, (ii) the associated drying stresses and (iii) crack initiation and propagation in both the timber and gluelines, would represent an economical and efficient method to investigate potential solutions (Angst and Malo 2010; Redman 2017). To establish a comprehensive delamination assessment model, it was necessary to collect the physical and mechanical properties of the SPG material and its associated gluelines. The SPG physical properties, such as permeability, diffusion coefficients and desorption-isotherm, have previously been described by Redman (2017). However, there is a lack of information regarding the mechanical properties, especially the fracture properties and their relationship to moisture content variation. In the literature, the continuum damage mechanics (Cheng et al. 2022; Gilbert et al. 2020; Kachanov 1986) and the cohesive zone method (Barenblatt 1962; Dugdale 1960) are the two most commonly used approaches to model the initiation and propagation of the cracks occurring during the delamination test (Fig. 1). Such models require the input of the Mode I (tension normal to the crack path) and Mode II (shear tangential to the crack path) fracture energies and corresponding crack initiation stresses (Franke and Quenneville 2011; Sandhaas 2012). Thus, these values had to be experimentally

measured to advance knowledge of the material behaviour of SPG and the fracture properties of hardwood in general.

This paper aims to determine the fracture properties of SPG sawn timber and its associated adhesive bonds (gluelines). As the mechanical properties of timber are known to be moisture sensitive (Ross 2010) and the SPG glulam moisture content varies during the delamination test of the AS/NZS 1328.1 (2011), the fracture properties along the crack paths experienced in the delamination tests were determined in this study at different moisture content levels (i.e., 8%, 12% and 16%). First, published test methods for measuring Mode I and II fracture energies were reviewed, and the most appropriate methods for timber were selected. Second, the Mode I and II fracture energies of the timber with a tangential-longitudinal (TL) crack system (i.e., with the crack occurring in the radial-longitudinal [RL] plane and propagating along the longitudinal direction) and the gluelines crack system (i.e., with the crack propagating along the glueline) at the different moisture content levels were experimentally measured. The shear strength in the RL plane needed to input crack initiation stress was estimated from the Mode II fracture tests. Statistical analyses were also conducted to examine the relationship between the moisture content and both the fracture energies and shear strengths. Third, as the previous fracture properties were found to be insensitive to moisture content variation (for the investigated moisture content range), and as the tensile strength perpendicular to the grain of SPG sawn timber is available in the literature, only the tensile strength normal to the glueline at the moisture content of 12% was measured. Finally, the fracture properties were also compared to the limited data on hardwood species.

Figure 2 shows the timber orientations in the tangential (T), radial (R) and longitudinal (L) directions. Figure 3 shows the crack systems investigated in this study.

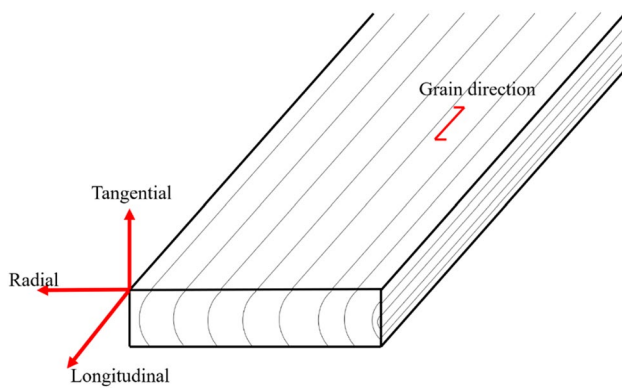


Fig. 2 Timber tangential (T), radial (R) and longitudinal (L) directions

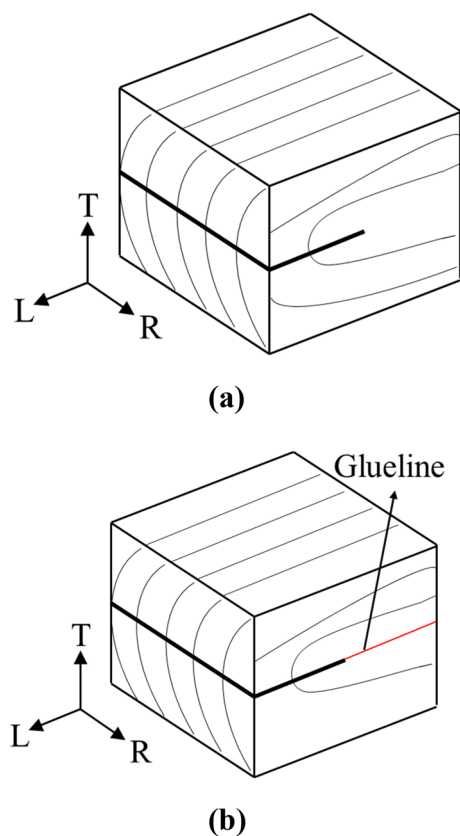


Fig. 3 Timber crack systems: **a** TL and **b** glueline

2 Fracture test methods and timber properties versus moisture content

The fracture energy describes the work done to separate a unit area of a crack entirely apart and is a fundamental material property when studying crack or delamination problems (Jensen et al. 2011). Three different fracture modes lead to crack developments: (1) Mode I, also referred to as

the ‘opening mode’ or ‘tension mode’, which describes the crack initiation and propagation in terms of a tension stress orthogonal to the crack path; (2) Mode II, also referred to as the ‘shearing mode’, which describes the shear stress in the plane of the crack induces the crack to develop and propagate; and (3) Mode III, also referred to as the ‘tearing mode’, which describes the crack occurs due to out-of-plane shear stress (Franke and Quenneville 2014). Various test setups have been used in the literature to capture the fracture energies of the different modes. The most commonly adopted methods for timber material are introduced and discussed in the next two subsections.

2.1 Fracture Mode I test methods

Different test methods have been used in the literature to measure the Mode I fracture energy of timber specimens. Ostapska and Malo (2020) applied the wedge-splitting test method proposed by Brühwiler and Wittmann (1990) for concrete to timber. This test method requires specimens with large fracture areas (Brühwiler and Wittmann 1990). Franke and Quenneville (2014) applied the compact tension shear (CTS) test setup, which was proposed by Richard and Benitz (1983), to radiata pine laminated veneer lumber (LVL) and sawn timber. The advantage of the CTS is that either Mode I, Mode II or mixed mode fracture energies can be measured with one test rig by changing the angle of the applied load. However, the CTS specimens must be carefully prepared with high accuracy to avoid any unsymmetrical loading; the applied stress and resulting fracture energy vary significantly (Franke and Quenneville 2014). In addition, De Moura et al. (2010) applied the double cantilever beam (DCB) test for fracture Mode I to *Pinus pinaster* sawn timber and stable crack propagation was achieved.

The method most commonly used to measure the Mode I fracture energy of timber samples was proposed by Gustafsson (1988) and has been used by Ardalany et al. (2012), Franke and Quenneville (2014) and Larsen and Gustafsson (1991). It is referred to as the single-end notched beam (SENB) specimen. A notched specimen is glued to two pieces of timber to form a beam. The specimen is loaded in three-point bending, forcing the crack to open and propagate. Due to the gluing involved in preparing the specimens, the manufacturing process is time-consuming if a large number of tests are required. Ardalany et al. (2012) improved the setup by replacing the side timber pieces with steel sections to which the notched timber specimens can easily be connected, significantly simplifying the manufacturing process. A counterbalance weight is placed on each steel section to offset the effect of the self-weight of the test rig into the calculations of the fracture energy. This method was adopted in this study because it is simple and commonly used for timber.

2.2 Fracture Mode II test methods

Unlike Mode I, Mode II fracture energy is more challenging to measure experimentally, especially due to unstable crack growth (Reiner et al. 2022). Various approaches have been described in the literature. For example, Yoshihara (2008) applied an asymmetric four-point bending test that is straightforward for fracture energy measuring. Wu (1967) tested centre cracked plate shear specimens; however, this test method is not valid for all timber species, as buckling might occur in the manufacturing process of the samples (Aicher et al. 1997; Wu 1967). Williams and Birch (1976) proposed a shear mode test by tensile loading; however, they encountered great difficulties in executing the tests.

Franke and Quenneville (2014) applied a variation of the compact shear specimen (CSS) proposed by Jones and Chisholm (1975) and Prokopski (1995) to measure the Mode II fracture energy of radiata pine LVL specimens. Two notches were cut symmetrically on the sides of the specimens, and a displacement-controlled load was applied to shear the middle part relative to the side ones. The CSS test has a relatively simple setup and always results in pure Mode II failure, even when the cracks do not propagate simultaneously above the two notches (Reiner et al. 2022). Thus, due to its simplicity and the fact that valid results can be obtained, the CSS was selected for the fracture Mode II tests.

2.3 Sensitivity of timber mechanical properties to moisture content

Many wood mechanical properties are known to be sensitive to the moisture content, with the properties increasing with decreasing moisture content below the fibre saturation point (Ross 2010). However, the relationship between wood moisture content and fracture behaviour, especially the fracture energies, is still under researched. Rug and Badstube (International Council for Building Research 1989) conducted fracture Mode I tests on red pine samples using the method proposed by Gustafsson (1988) at different moisture content levels ranging from about 10–23% and reported that moisture content had no significant effect on Mode I fracture energy. Conversely, Reiterer and Tschegg (2002) applied the wedge-splitting method to measure the Mode I fracture energy of spruce sawn wood at about 7%, 12%, 18% and 55% of moisture content and found that as the moisture content increased, the fracture energy increased.

3 Methodology

3.1 General

Australia's native forest SPG boards, with the trees harvested in QLD, were used to analyse the sensitivity of the fracture

properties to the moisture content. The boards were 25 mm thick and were machined to 22 mm before gluing (for further details, see paragraph three). After the drying process of the delamination test (AS/NZS 1328.1, 2011), the cracks typically developed normal to the tangential direction and along the gluelines, as shown in Fig. 1. Thus, the Mode I and II fracture energies in the TL and glueline crack systems were investigated as part of this study.

When the boards needed to be glued to manufacture the samples (as detailed in Sect. 3.2 and 3.3), the boards were bonded in accordance with the results of Leggate et al. 2020, 2021b, (2022) to maximise adhesion. Specifically, the boards were face milled to a thickness of 22 mm to activate the surface and the commercial resorcinol-formaldehyde (RF) adhesive manufactured by Jowat Adhesive was used. The gluing process consisted of: (1) mixing the resorcinol with formaldehyde by 4:1 for five minutes and letting it stand for 10 min; (2) face milling the surfaces to be glued with a Rotoles 400 D-S manufactured by Ledinek (Leggate et al. 2021a); (3) manually applying the adhesive onto the milled surfaces immediately after milling at a glue spread rate of 450 g/m²; and (4) pressing the boards together under a pressure of 1.4 MPa for 12 h. Before the gluing process described above took place, the boards were conditioned at 20 °C and 65% relative humidity.

After the gluing process was finished and the glue was fully cured (a minimum period of 24 h after gluing), the samples were placed in different conditioning chambers with targeted equilibrium moisture content of 8%, 12% and 16%, corresponding to the conditioning chambers set at 20 °C/40% relative humidity (RH), 20 °C/65% RH and 60 °C/90% RH, respectively (Commonwealth Scientific and Industrial Research Organisation, 1977). The samples were conditioned until they reached moisture equilibrium consisting of a mass change of less than 0.2% over a 24-h period (AS/NZS 1080.1, 2012). The samples were conditioned for about 12, 4 and 12 weeks at 8%, 12% and 16% of equilibrium moisture content, respectively. The moisture contents were selected based on measurements of the glulam samples during delamination tests that reached a moisture content as high as 16% after vacuum impregnation and as low as 8% after kiln drying. However, as discussed further in the Results section, the fracture energies and shear strength were not sensitive to the variations in moisture content. As a result, the samples for tensile strength were only conditioned at a targeted moisture content of 12%.

Immediately after testing, the actual moisture content of each sample was determined using the oven-dry method of the AS/NZS 1080.1 (2012).

The overview of experimental samples is summarised in Table 1, including the number of samples and sample names. Twice the amount of samples were prepared for the glueline crack system than the TL crack system due to the potentially

Table 1 Summary of samples' information

| Test | Sample name | Moisture content (%) | Number of samples |
|---|-----------------|----------------------|-------------------|
| Fracture Mode I TL crack system | MI-8%-TL | 8 | 10 |
| | MI-12%-TL | 12 | 10 |
| | MI-16%-TL | 16 | 10 |
| Fracture Mode I Glueline crack system | MI-8%-Glueline | 8 | 20 |
| | MI-12%-Glueline | 12 | 20 |
| | MI-16%-Glueline | 16 | 20 |
| Fracture Mode II TL crack system | MI-8%-TL | 8 | 10 |
| | MI-12%-TL | 12 | 10 |
| | MI-16%-TL | 16 | 10 |
| Fracture Mode II Glue- line crack system | MI-8%-Glueline | 8 | 20 |
| | MI-12%-Glueline | 12 | 20 |
| | MI-16%-Glueline | 16 | 20 |
| Tensile strength | T-12%-Glueline | 12 | 20 |

higher variability in the test results. All the TL or glueline samples were cut and prepared from different boards to ensure the results were not biased towards one board.

After the fracture properties were obtained, one-way analysis of variance (ANOVA) statistical analyses were conducted to determine whether there were any statistically significant differences between the different moisture content groups. If a critical value was not reached in one-way ANOVA, it was concluded that a given fracture property was unrelated to the moisture content of the sample.

3.2 Mode I fracture tests

As mentioned above, the three-point bending test setup proposed by Gustafsson (1988) was used to measure the Mode I fracture energy due to its effectiveness and ease of implementation. The Mode I tested samples are presented in Fig. 4a for the TL crack system and Fig. 4b for the glueline crack system. In Fig. 4a, 100 (deep) × 90 (wide) × 44 mm (thick) samples were produced. To produce the 44-mm thick samples from the 22-mm thick boards, two SPG pieces, cut from the same overall board, were face glued together. The grain orientations of all boards were selected such that the cracks were developed in the chosen system, with the orientation shown in Fig. 4a. All the specimens were manufactured from different overall boards. For each sample, (1) a 5 (thick) × 60 mm (deep) notch was cut by a V-shaped blade in the middle of the sample from which the crack could initiate and (2) two 25-mm deep side notches were cut to connect the sample to the test rig shown in Fig. 5 (photo) and Fig. 6 (schematic).

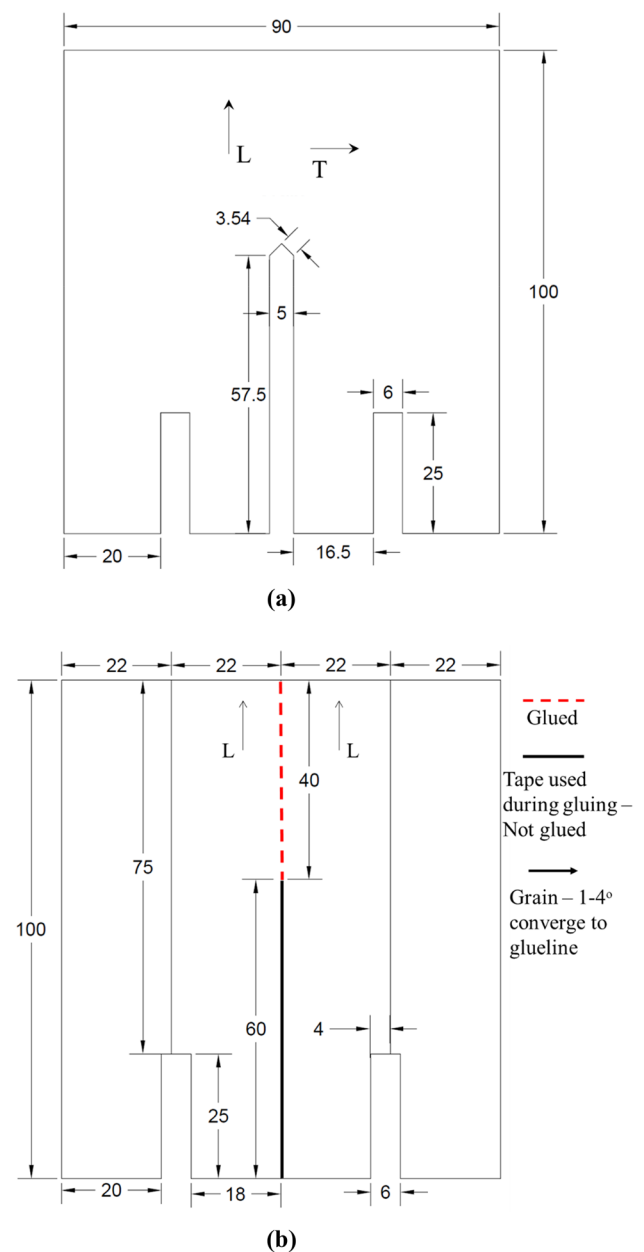


Fig. 4 Sample geometry of Fracture Mode I in **a** the TL and **b** glueline crack systems (units in mm)

In Fig. 4b for the glueline crack system samples, four 22-mm thick pieces were glued together to form an 88-mm thick glulam. The two middle pieces came from the same overall board and were selected to have the grain orientation relative to the glueline making an angle of 1° to 4° and converging towards the glueline. This configuration encouraged the crack to propagate along the glueline as explained by Ammann and Niemz (2015) and Komatsu et al. (1974). All the specimens were manufactured from different overall boards. A thin adhesive tape was positioned over 60 mm on

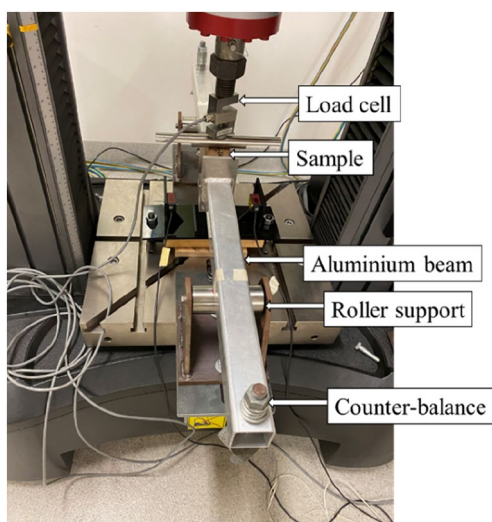


Fig. 5 Experimental setup for fracture Mode I

the two middle pieces before gluing to prevent adhesion and create a notch equivalent to the samples shown in Fig. 4a and from where the crack could propagate. The produced samples were 100 (deep) × 88 (wide) × 44 mm (thick) sample with the orientation shown in Fig. 4b. Two 25-mm deep side notches were cut to connect the sample to the test rig as shown in the Fig. 4b.

The samples were then connected to two aluminium beams, as shown in Figs. 5 and 6 to form a beam. The beam was positioned on two roller supports to be loaded in three-point bending in a 100 kN capacity INSTRON universal testing machine fitted with a 2.5 kN load cell. A half-round was connected to the load cell to load the specimens at mid-span. Counterbalance weights were also used at the extremity of the aluminium beams to offset both the self-weight of the timber samples and the beams themselves.

A loading rate of 8 and 1.2 mm/min was selected for the TL and glueline crack system samples, respectively, to target failure in three to five minutes.

The Mode I fracture energy G_{I_f} was calculated as (Larsen and Gustafsson 1991; Rug et al. 1990),

$$G_{I_f} = \frac{Q}{h_c b} \quad (1)$$

where Q is the work performed to fully fracture the sample and calculated from the load-displacement curve, h_c is the measured depth of the specimen above the crack tip and b is the measured specimen thickness (Larsen and Gustafsson 1991; Rug et al. 1990). The displacement was measured at the stroke of the testing machine. It should be noted that despite the fact that the displacement provided by the testing machine may differ from the actual displacement of the specimens, as outlined by Gilbert et al. (2022), the testing machine behaves linearly and the work performed by the testing machine is equal to the work needed to fully fracture the samples.

3.3 Mode II fracture tests

As previously discussed, the compact shear test setup was selected for the Mode II fracture tests due to its ease of implementation and common use in timber research (Cramer and Pugel 1987; Franke and Quenneville 2014; Jones and Chisholm 1975; Prokopski 1995; Reiner et al. 2022). The tested specimens for the TL (100 (deep) × 90 (wide) × 44 mm (thick) and glueline (100 (deep) × 88 (wide) × 44 mm (thick) crack systems are shown in Fig. 7a and b, respectively. The former samples comprised two 22-mm thick boards face glued together in which two notches, from which the cracks can initiate, were cut by a V-shaped blade, as shown in Fig. 7a. The latter samples were manufactured from four glued 22-mm thick boards. Similar to the Mode

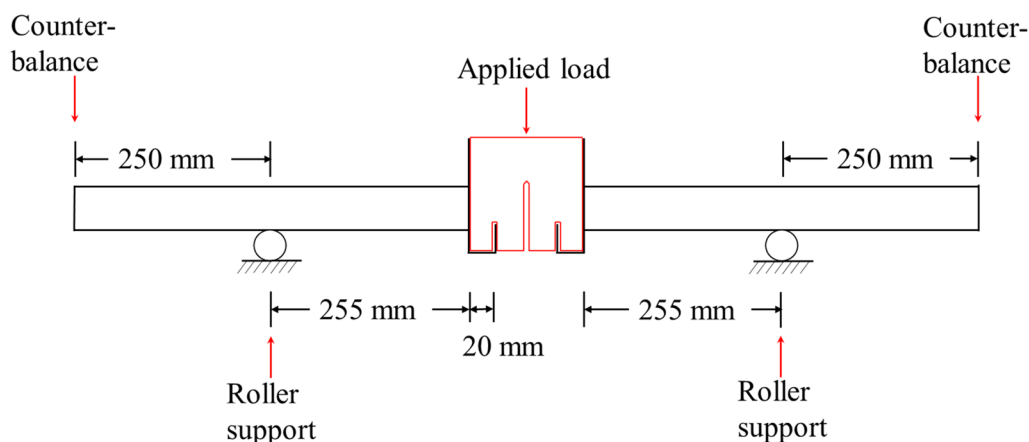


Fig. 6 Fracture Mode I test setup sketch

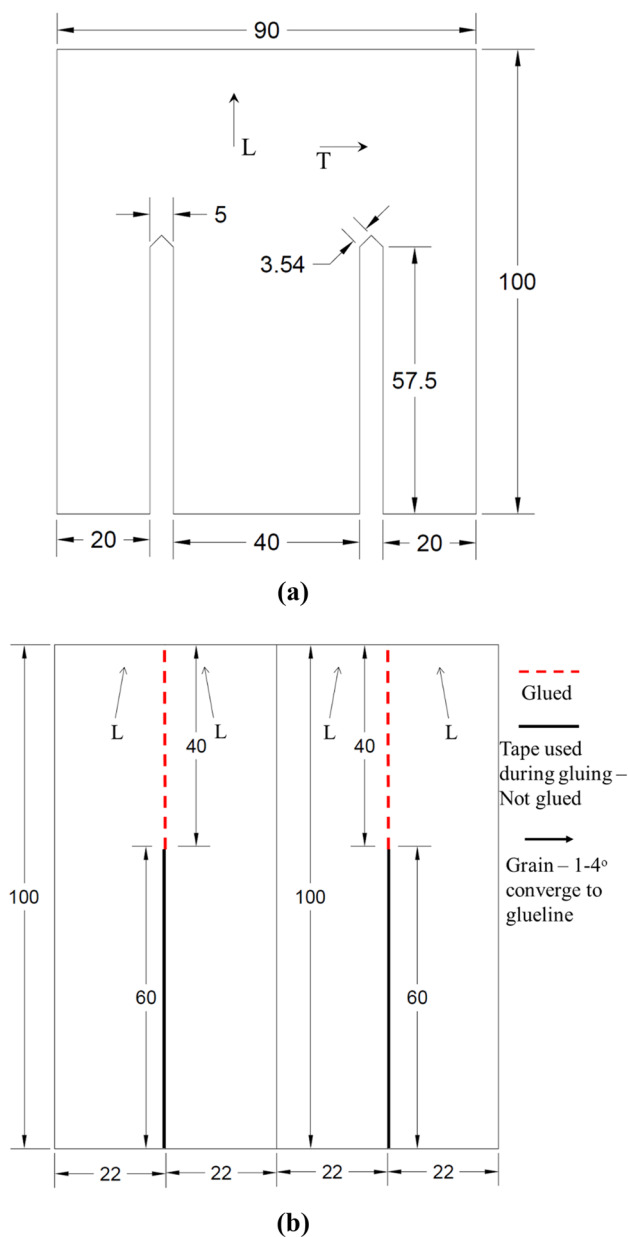


Fig. 7 Sample geometry of Fracture Mode II in **a** the TL and **b** glue-line crack systems (units in mm)

I samples, a thin adhesive tape was positioned between the boards, as shown in Fig. 7b, to prevent adhesion and create equivalent type notches for crack initiation. All four boards used per specimen were cut from the same overall board, and all specimens were prepared from different overall boards. All the boards were chosen to have the grain making an angle of 1–4 degrees to the glue-lines as described in Sect. 3.2 and shown in Fig. 7b. It should be noted that the

same overall board was used to manufacture one specimen to obtain specimens with consistent material properties.

The Mode II fracture test setup is shown in Fig. 8. The specimens were positioned in a 100 kN INSTRON universal testing machine and tested in displacement control at a stroke rate of 0.8 and 0.3 mm/min for the TL and glue-line crack systems, respectively, to best achieve failure in three to five minutes. Two steel blocks were positioned as supports at the base of the specimens, and another 40-mm wide steel block was placed in the middle of the specimen and acted as the loading block.

The Mode II fracture energy $G_{II\bar{f}}$ was calculated as (Larsen and Gustafsson 1991; Rug et al. 1990),

$$G_{II\bar{f}} = \frac{Q}{2h_c b} \tag{2}$$

where Q is the work needed to fully fracture the sample and calculated from the load-displacement curve, h_c is the measured depth of the specimen above the crack tip and b is the measured thickness of the specimen (Larsen and Gustafsson 1991; Rug et al. 1990). The displacement was recorded from the stroke of the testing machine.

Additionally, the shear strength τ_s of the material was estimated from the Mode II test as,

$$\tau_s = \frac{F_{max}}{2h_c b} \tag{3}$$

where F_{max} is the maximum recorded applied load.

3.4 Tensile strength tests

The tensile strength perpendicular to the grain was determined following the procedure in the American Society for Testing and Materials (ASTM) D143-22 (2022). The test setup and specimen details are shown in Figs. 9 and 10, respectively. The specimens were positioned in a custom-made rig (Fig. 9) and tested in displacement control at a stroke rate of 0.5 mm/min to best achieve failure in three to five minutes, in a 30 kN INSTRON universal testing machine. The tensile strength σ_t was calculated as the maximum load divided by the measured minimum cross-section area of the specimen.

As the Mode I and II fracture energies and shear strength were found to be insensitive to moisture content variations for the investigated range (see Sect. 4.1 and 4.2), only the tensile strength at a targeted moisture content of 12% was measured. Additionally, as the same test setup was applied to 28 sawn SPG samples in Leka (2022), only the tensile strength of the glue-line was measured in this study. Leka’s (2022) results are reported in Sect. 4 for information

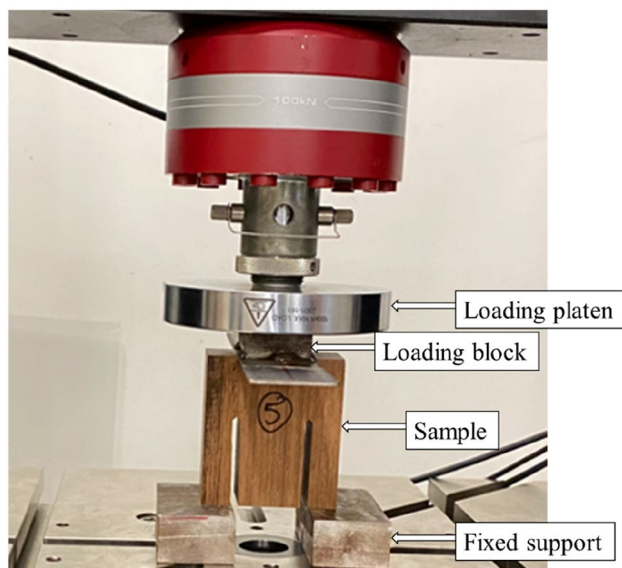


Fig. 8 Experimental setup for fracture Mode II.

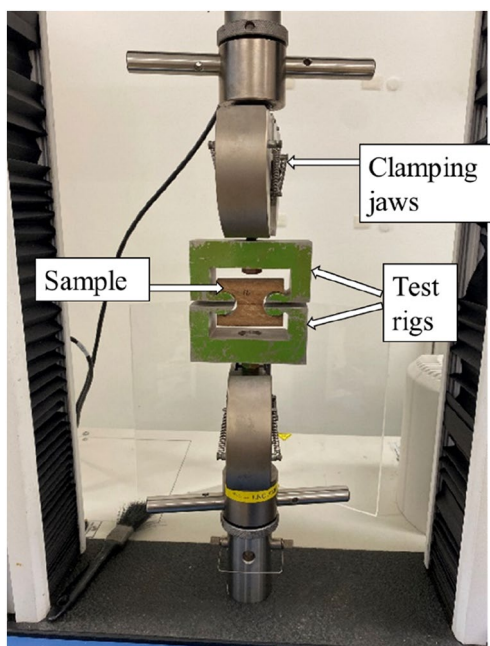


Fig. 9 Tensile strength test setup

purposes and to provide a comparison to the glueline samples. All the specimens were glued from two pieces cut from the same overall board, and all the specimens were manufactured from different overall boards.

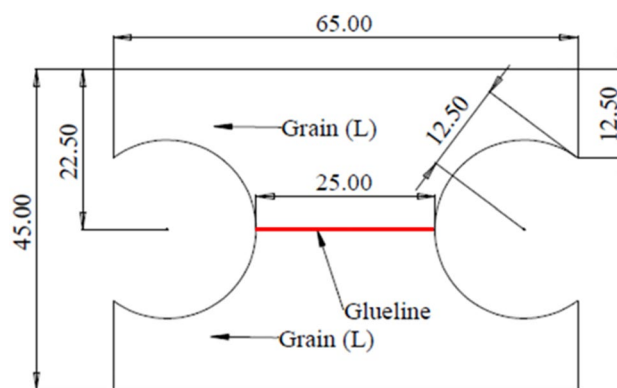


Fig. 10 Sample geometry of the tensile strength test

4 Results and discussion

4.1 Mode I fracture test results

The stress-displacement curves for all the fracture Mode I tests relative to the different crack systems and moisture contents are presented in Fig. 11. The nominal and actual moisture contents and average measured fracture energies, with the associated coefficient of variation (CoV), are summarised in Table 2. The Mode I fracture energy in the TL crack system was about four times higher than that in the glueline crack system, which indicated that crack propagated faster in the glueline than the timber.

The results of the one-way ANOVA statistical analyses of the different moisture content groups showed that the fracture energies for (1) the TL crack system were: $F(227) = 0.318$, $p = 0.7301$, and (2) the glueline crack system were: $F(257) = 1.913$, $p = 0.157$. Thus, there was no statistically significant difference between the group means for both the TL and glueline crack systems and the Mode I fracture energy was independent of the range of moisture content analysed for both systems. This result also indicated that the Mode I fracture energy did not appear to follow the same trend as the ‘common’ mechanical properties that vary with the moisture content. According to Guitard (1987), the difference in mechanical properties between 8% and 16% moisture content levels would be 27%.

Since the Mode I fracture energy in both the TL and glueline crack systems was not statistically sensitive to moisture content, the average value fracture energy of the three moisture content groups could be used as future numerical model input to simulate the delamination test of the AS/NZS 1328.1 (2011).

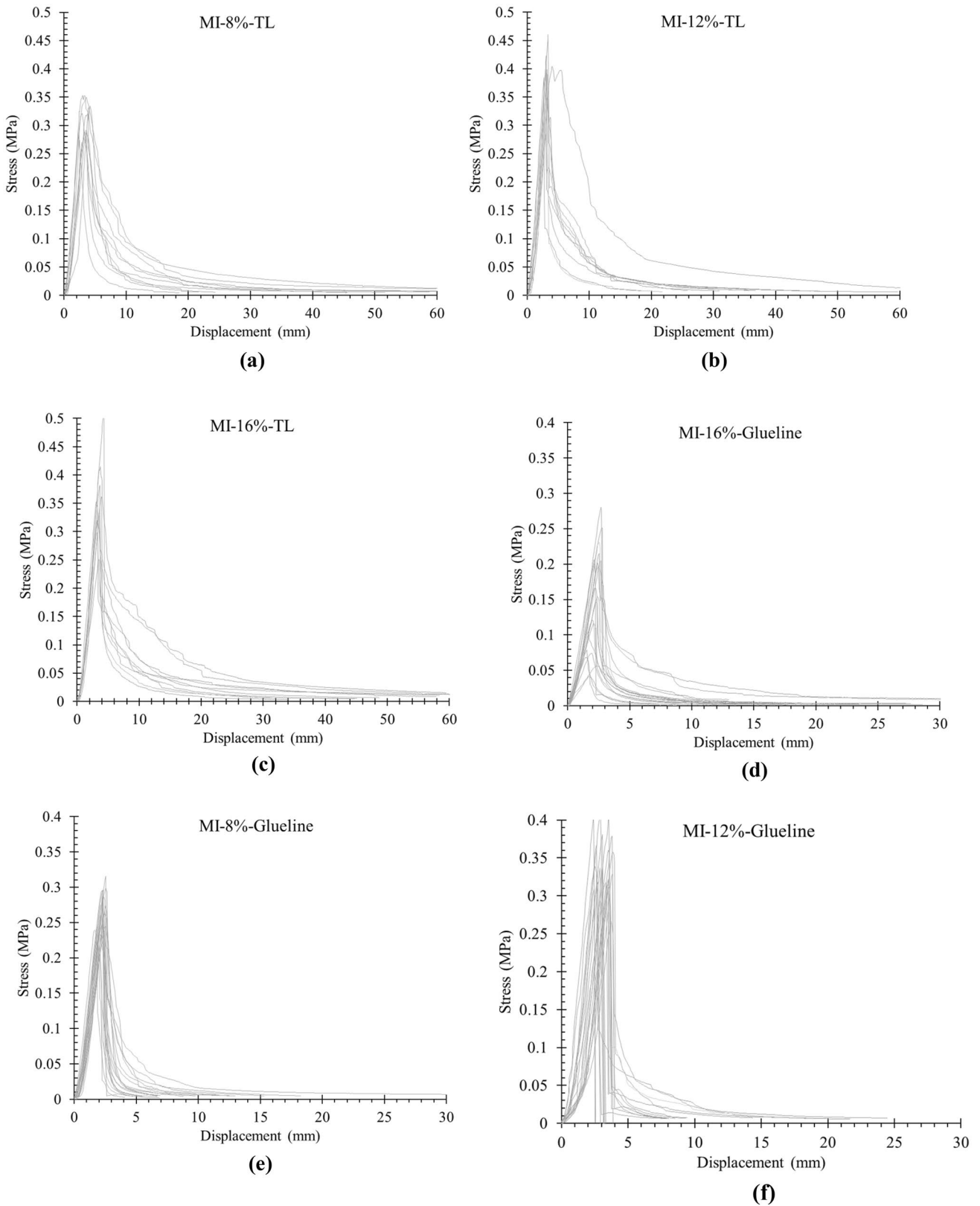


Fig. 11 Stress-displacement curves for the Mode I fracture energy tests for TL crack system at **a** 8%, **b** 12% and **c** 16% moisture content, and glueline crack system at **d** 8%, **e** 12% and **f** 16% moisture content

Table 2 Mode I fracture test results

| Crack system | Moisture content | | | Fracture energy G_{Iff} | | |
|--------------|------------------|------------|---------|---------------------------|----------------|---------|
| | Nominal (%) | Actual (%) | CoV (%) | Number of tests | Average (N/mm) | CoV (%) |
| TL | 8 | 8.3 | 2.2 | 10 | 1.99 | 44.4 |
| | 12 | 12.5 | 2.3 | 10 | 2.02 | 55.5 |
| | 16 | 15.8 | 2.0 | 10 | 2.31 | 42.6 |
| Glueline | 8 | 8.2 | 3.5 | 20 | 0.46 | 38.1 |
| | 12 | 12.4 | 1.9 | 20 | 0.56 | 32.0 |
| | 16 | 16.1 | 1.6 | 20 | 0.42 | 49.6 |

Figure 12 shows the typical failure modes for the Mode I fracture tests. The cracks initiated at the tip of the notch or non-glued area and propagated up straight or along the glueline for the TL and glueline system samples, respectively.

4.2 Fracture Mode II test results

The stress-displacement curves for all the Mode II fracture tests relative to the crack systems and moisture contents are shown in Fig. 13. The nominal and actual moisture contents, average fracture energies and maximum stresses, with the associated CoV, are summarised in Table 3. Unlike the Mode I fracture tests, the curves typically displayed two local maximums, corresponding to one side of the sample failing first and the load redistributing to the other side until a crack eventually propagated on the other side (Reiner et al. 2022).

As mentioned in the introduction, the maximum stress from Mode II fracture tests was used as model input for the Mode II crack initiation. Thus, the statistical analyses were conducted for both fracture energy and shear strength to determine whether these properties were sensitive to the moisture content variation. The one-way ANOVA results for (1) the TL system fracture energy were: $F(227) = 2.411$, $p = 0.109$; (2) the glueline systems fracture energy were: $F(257) = 2.670$, $p = 0.078$; (3) the TL system shear strength were: $F(227) = 2.566$, $p = 0.095$; and (4) the glueline system shear strength were: $F(257) = 0.342$, $p = 0.712$. There was no statistically significant difference between the group means for the Mode II fracture energy and maximum stress for both the studied crack systems. Thus, these fracture properties were independent of the moisture content for the range analysed and the Mode II fracture properties could be taken as constant input data in delamination test modelling.

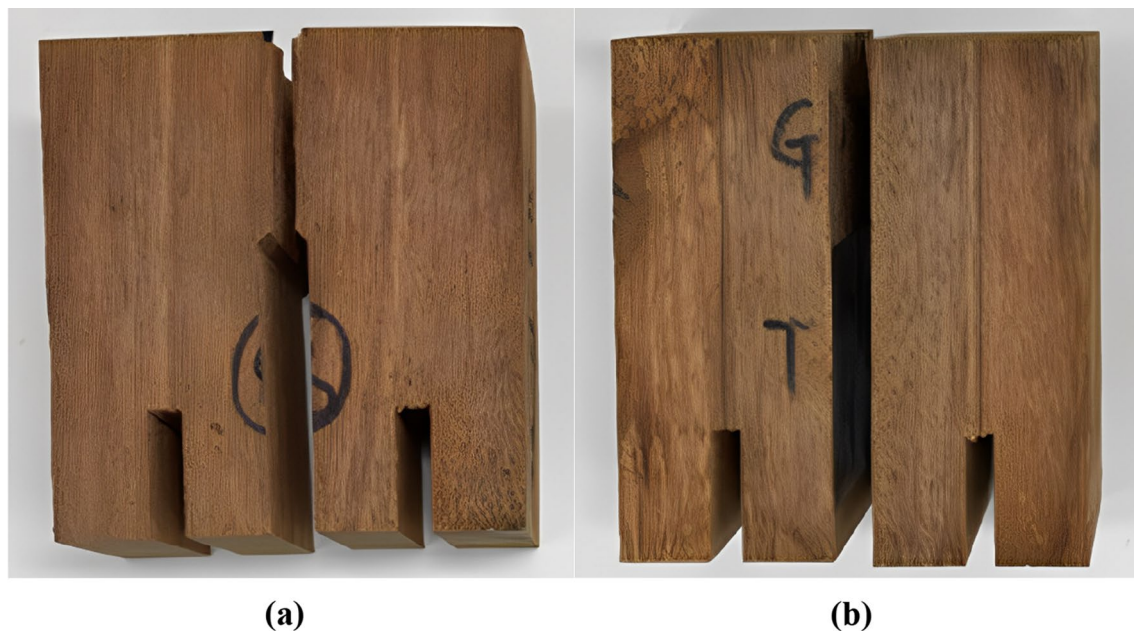


Fig. 12 Fracture Mode I typical failure modes for **a** TL and **b** glueline crack systems

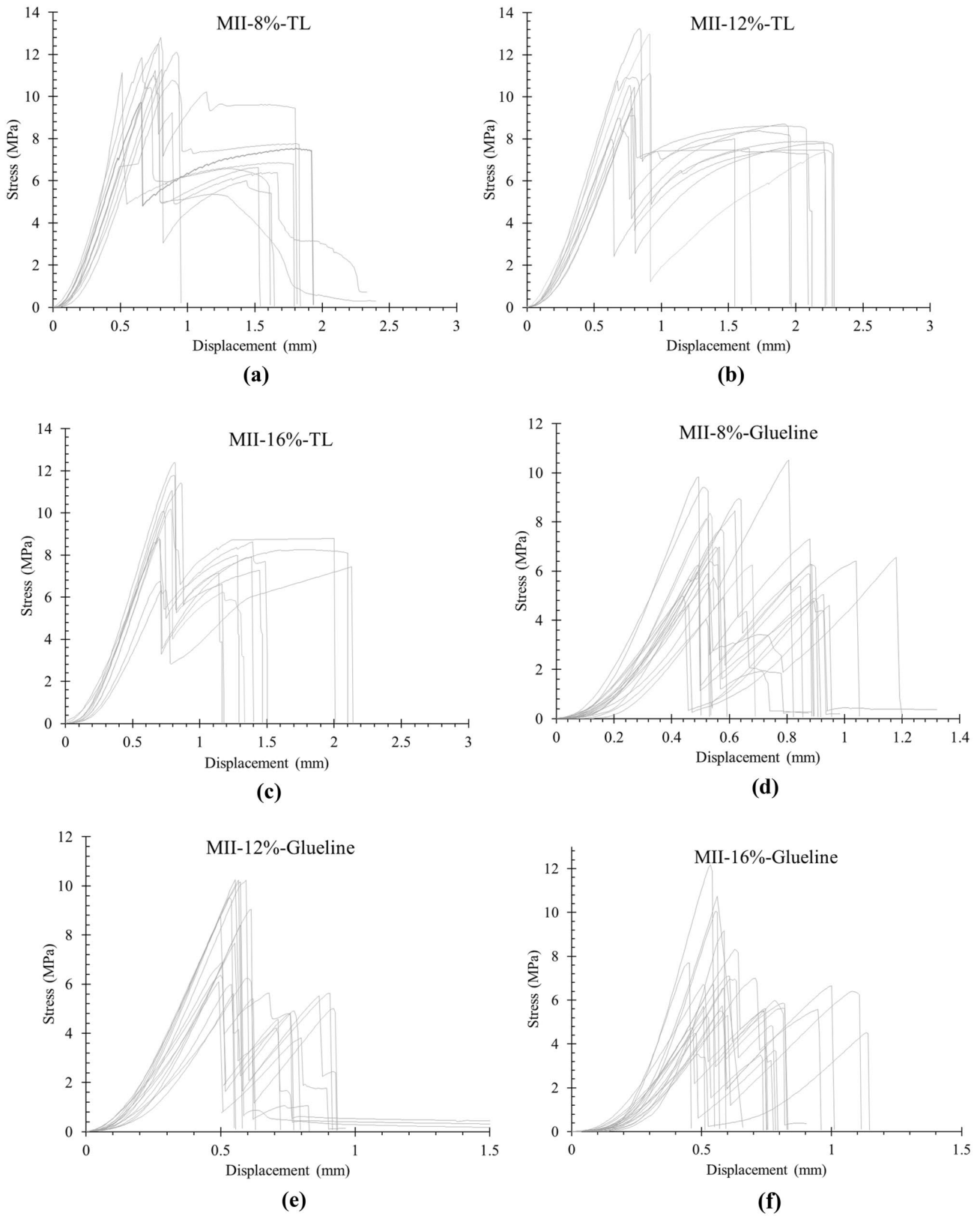


Fig. 13 Stress-displacement curves for the Mode II fracture energy tests for TL crack system at **a** 8%, **b** 12% and **c** 16% moisture content, and glueline crack system at **d** 8%, **e** 12% and **f** 16% moisture content

Table 3 Fracture Mode II test results

| Crack system | Moisture content | | | Fracture properties | | | | |
|--------------|------------------|------------|---------|---------------------|--------------------------|---------|-------------------------|---------|
| | Nominal (%) | Actual (%) | CoV (%) | Number of tests | Fracture energy G_{II} | | Maximum stress τ_s | |
| | | | | | Average (N/mm) | CoV (%) | Average (MPa) | CoV (%) |
| TL | 8 | 8.1 | 2.4 | 10 | 10.94 | 26.4 | 9.88 | 19.3 |
| | 12 | 12.5 | 1.8 | 10 | 12.17 | 16.0 | 10.48 | 16.2 |
| | 16 | 15.7 | 3.6 | 10 | 10.33 | 26.1 | 11.44 | 8.9 |
| Glueline | 8 | 8.4 | 3.2 | 20 | 2.73 | 23.8 | 7.23 | 26.0 |
| | 12 | 12.4 | 2.2 | 20 | 2.51 | 27.2 | 7.64 | 24.5 |
| | 16 | 16.3 | 1.7 | 20 | 2.39 | 22.1 | 7.20 | 28.2 |

As Table 3 shows, the shear strength of the sawn timber was about 1.4 times higher than that of the glueline, which indicated that the shear cracks initiated in the glueline and not in the timber. Additionally, as the Mode II fracture energy was more than four times higher in the TL crack system than the glueline, cracks also propagated faster in the gluelines.

Figure 14 shows the typical failure modes for the fracture Mode II tests. The cracks initiated at the tip of notches or non-glued area and propagated straight up, which correlated to the designed crack paths.

4.3 Tensile strength test results

As mentioned above, and shown earlier, as the fracture energies and shear strengths were found to be insensitive to the moisture content variations, the tension samples were only tested at a targeted moisture content of 12%. The average test results, with the associated CoV, are summarised in Table 4. Leka's (2022) results on native SPG sawn timber are also summarised in Table 4 for comparison purposes. The typical tensile failure mode of the glued samples is shown in Fig. 15, which shows that the failure principally occurred in the glueline.

The average tensile strength perpendicular to the grain of the sawn material in Leka's (2022) study was 56% lower

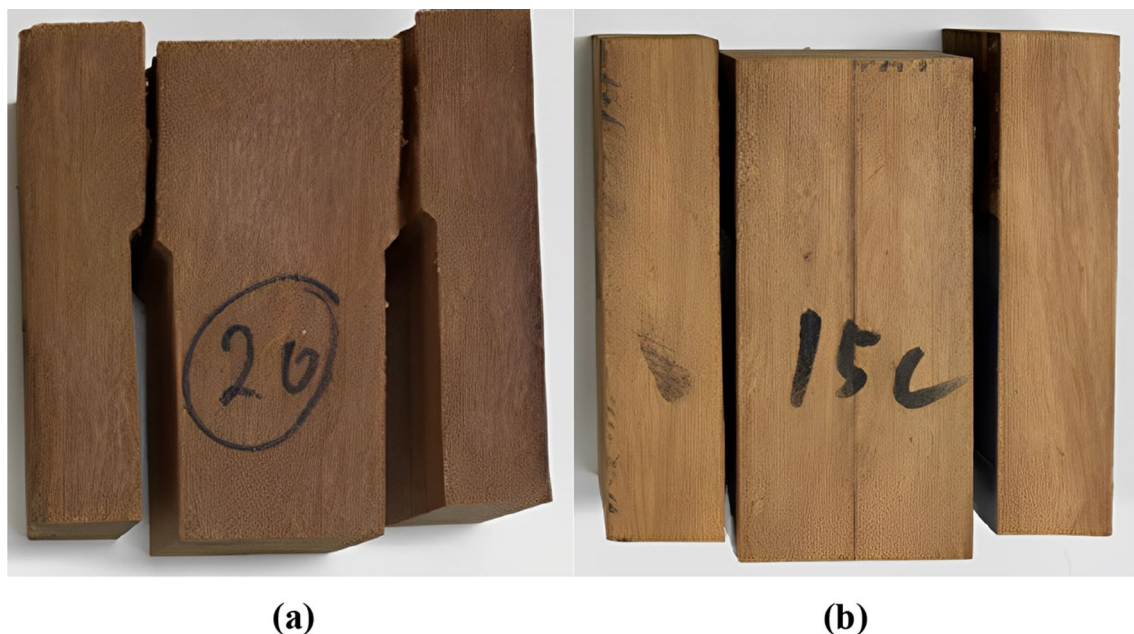
**Fig. 14** Fracture Mode II typical failure modes for **a** TL and **b** glueline crack systems

Table 4 Glueline tensile strength tests results

| Test | Moisture content | | | Tensile strength σ_t | | |
|-------------------------|------------------|------------|---------|-----------------------------|---------------|---------|
| | Nominal (%) | Actual (%) | CoV (%) | Number of tests | Average (MPa) | CoV (%) |
| Glueline | 12 | 12.7 | 2.8 | 20 | 6.81 | 19.9 |
| Sawn timber (Leka 2022) | 12 | 13.3 | 5.1 | 28 | 4.37 | 22.4 |

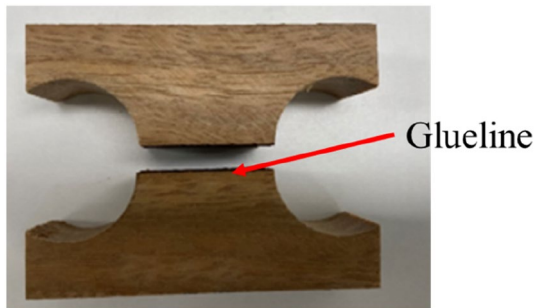


Fig. 15 Typical failure Mode of the glued samples in tension

than the glueline strength measured in this study. However, since failure occurred in the glueline (Fig. 15), the glueline tensile strength should be lower than that in the timber (otherwise timber failure would have been observed). This contradiction could be linked to the natural variability of the timber material and the boards being sourced at different times. Indeed, despite the material being SPG from native QLD forests, the logs might have been harvested from different sites. No significant difference in the density of the specimens in this study (average density of 1037.48 kg/m³) and in Leka’s study (2022) (average density of 1024.59 kg/m³) was observed.

4.4 Discussion

Table 5 compares the fracture test results to the results of published studies on hardwood species. For Mode I in both the TL and RL crack systems all together, Leka (2022) applied the same test setup to the same material studied examined in this study. The fracture energy was 27.5% lower than that reported in this study. This difference might have arisen because (1) Leka (2022) did not make any distinction between the tangential and radial directions of the timber, with the TL and RL crack systems having different fracture energies; and (2) the natural variability in the timber as discussed in Sect. 3.4. Compared to reported fracture energies on other hardwood species, the fracture energy in this study was higher, which might be due to the high density of the native forest SPG, which is higher than 1000 kg/m³ (Redman 2017). Frühmann (2002) measured the Mode I fracture energy of sawn beech boards in the TL crack system by applying a wedge-splitting test. The resulting fracture energy was nearly three times lower than that measured in this study. Reiterer et al. (2000) also used the wedge-splitting test to measure the Mode I fracture energy of oak and ash sawn boards in the RL crack system, and the resulting fracture energies were only 10.9% and 17.5% lower, respectively, than the Mode I fracture energy found in this study.

Table 5 Fracture test results from other studies

| Fracture Mode | Species/type | Test setup | Crack system | Fracture energy (N/mm) | Reference |
|---------------|-------------------|-------------------------------|--------------|------------------------|--|
| Mode I | SPG sawn boards | Three-point-bending | TL | 2.11 | This study |
| | SPG sawn boards | Three-point-bending | TL/RL | 1.53 | Leka (2022) |
| | Beech sawn boards | Splitting test | TL | 0.73 | Frühmann (2002) and Frühmann et al. (2002) |
| | Oak sawn boards | Splitting test | RL | 0.23 | Reiterer et al. (2000) |
| | Ash sawn boards | Splitting test | RL | 0.37 | Reiterer et al. (2000) |
| | SPG gluelines | Three-point-bending | Glueline | 0.48 | This study |
| | Beech gluelines | DCB | Glueline | 1.00 | Ammann and Niemz (2015) |
| Mode II | SPG sawn boards | CSS | TL | 11.16 | This study |
| | SPG sawn boards | CSS | TL/RL | 8.95 | Leka (2022) |
| | Beech sawn boards | Notched bending beam specimen | RL | 1.79 | Frühmann et al. (2002) |

Ammann and Niemz (2015) conducted glueline fracture tests on European beech glulam, with boards bonded by RF adhesive as in the present study. The glueline fracture energy of this study was about half that found by Ammann and Niemz (2015). This is likely because better bonds were achieved by Ammann and Niemz (2015), who found that over 50% of tests failed in the timber rather than the gluelines.

For Mode II in the TL crack system, the fracture energy from this study was 24.7% higher than that reported by Leka (2022) with the same material. However, for Mode I, no distinction between the RL and TL crack systems was made by Leka (2022). Frühmann et al. (2002) tested the Mode II fracture energy of sawn beech boards in the RL crack system using notched bending beam specimens, and the fracture energy was about six times lower than that reported in this study.

Additionally, this study showed that the fracture energy of SPG for Mode II was about five times higher than that for Mode I, for both the TL and glueline crack systems.

5 Conclusion

The fracture properties of SPG sawn timber and associated adhesive bonds were measured at various moisture content levels. The properties included the Mode I and II fracture energies in the TL and glueline crack systems, the tension perpendicular to the grain and the shear strengths of the timber and gluelines. The sensitivity of these properties to the moisture content variations was analysed statistically. The study showed that the fracture properties were not correlated to the change of moisture content for the range investigated (i.e., between 8% and 16%). The average Mode I fracture energies in the TL and glueline crack systems were 2.1 N/mm and 0.48 N/mm, respectively. For the same crack systems, the average Mode II fracture energies were 11.2 (TL) and 2.5 N/mm (glueline). These values indicated that the cracks propagated faster in the gluelines than the timber. Additionally, the average shear strength was 10.6 MPa for the sawn material and 7.4 MPa for gluelines, which indicated that Mode II cracks initiated in the gluelines rather than the timber. The glueline tensile strength perpendicular to the grain was measured as 6.8 MPa at a moisture content of 12%, which is a value larger than that reported in the literature for the SPG sawn timber of 4.37 MPa. All the fracture properties measured in this paper could be used to model crack initiation and the propagation of SPG glulam subjected to wetting and drying.

Acknowledgements The authors would like to thank the technical team at the Salisbury Research Facility of the Queensland Department of

Agriculture and Fisheries (DAF) for helping with the specimen preparation and the technical team at Griffith University for manufacturing the testing jigs.

Author contributions PL: Conceptualization, Methodology, Sample manufacturing, Experiment, Analysis, Writing, Visualization. BPG: Conceptualization, Methodology, Experiment, Analysis, Writing, Revision, Visualization, Supervision. CK: Conceptualization, Methodology, Sample manufacturing, Revision, Supervision. RLM: Conceptualization, Sample manufacturing, Revision, Supervision. HK: Conceptualization, Revision, Supervision.

Funding Open Access funding enabled and organized by CAUL and its Member Institutions. This research was supported by the Australian Centre for International Agricultural Research, project FST/2019/128.

Data availability The data are available upon request.

Declarations

Conflict of interest The authors have no conflict of interest to declare.

Open Access This article is licensed under a Creative Commons Attribution 4.0 International License, which permits use, sharing, adaptation, distribution and reproduction in any medium or format, as long as you give appropriate credit to the original author(s) and the source, provide a link to the Creative Commons licence, and indicate if changes were made. The images or other third party material in this article are included in the article's Creative Commons licence, unless indicated otherwise in a credit line to the material. If material is not included in the article's Creative Commons licence and your intended use is not permitted by statutory regulation or exceeds the permitted use, you will need to obtain permission directly from the copyright holder. To view a copy of this licence, visit <http://creativecommons.org/licenses/by/4.0/>.

References

- Aicher S, Boström L, Gierl M, Kretschmann D, Valentin G (1997) Determination of fracture energy of wood in mode II. RILEM TC 133 report. Swedish National Testing and Research Institute, sweden
- American Society for Testing and Materials (ASTM) (2022) Standard test methods for small clear specimens of timber (ATSM D143–22). ASTM Int. <https://doi.org/10.1520/D0143-22>
- Ammann S, Niemz P (2015) Specific fracture energy at glue joints in european beech wood. *Int J Adhes Adhes* 60:47–53. <https://doi.org/10.1016/j.ijadhadh.2015.03.007>
- Angst V, Malo KA (2010) Moisture induced stresses perpendicular to the grain in glulam: review and evaluation of the relative importance of models and parameters. *Holzforschung* 64:609–617. <https://doi.org/10.1515/hf.2010.089>
- Ardalany M, Deam B, Fragiaco M (2012) Experimental results of fracture energy and fracture toughness of radiata pine laminated veneer lumber (LVL) in mode I (opening). *Mater Struct* 45(8):1189–1205. <https://doi.org/10.1617/s11527-012-9826-1>
- Australian and New Zealand Standard (AS/NZS) (2011) Glued laminated structural timber Part 1: Performance requirements and minimum production requirements (AS/NZS 1328.1). Standards Australia, Australia
- Australian and New Zealand Standard (AS/NZS) (2012) Timber-methods of test Method 1: Moisture content (AS/NZS 1080.1). Standards Australia, Australia

- Barenblatt GI (1962) The mathematical theory of equilibrium cracks in brittle fracture. *Adv Appl Mech* 7:55–129. [https://doi.org/10.1016/S0065-2156\(08\)70121-2](https://doi.org/10.1016/S0065-2156(08)70121-2)
- Bootle KR (1983) *Wood in Australia. Types, properties and uses.* McGraw-Hill, Noida
- Brühwiler E, Wittmann F (1990) The wedge splitting test, a new method of performing stable fracture mechanics tests. *Eng Fract Mech* 35(1–3):117–125. [https://doi.org/10.1016/0013-7944\(90\)90189](https://doi.org/10.1016/0013-7944(90)90189)
- Cheng X, Gilbert BP, Guan H, Dias-da-Costa D, Karampour H (2022) Influence of the earthquake and progressive collapse strain rate on the structural response of timber dowel type connections through finite element modelling. *J Build Eng* 57:104953. <https://doi.org/10.1016/j.jobte.2022.104953>
- Commonwealth Scientific and Industrial Research Organisation (CSIRO) (1977) Decay of timber flooring. Information Service, Sheet No 10–36, Division of Building Research, Highett
- Cramer SM, Pugel AD (1987) Compact shear specimen for wood mode II fracture investigations. *Int J Fract* 35:163–174. <https://doi.org/10.1007/BF00015586>
- De Moura M, Oliveira J, Morais J, Xavier J (2010) Mixed-mode I/II wood fracture characterisation using the mixed-mode bending test. *Eng Fract Mech* 77(1):144–152. <https://doi.org/10.1016/j.engfracmech.2009.09.014>
- Dugdale DS (1960) Yielding of steel sheets containing slits. *J Mech Phys Solids* 8(2):100–104. [https://doi.org/10.1016/0022-5096\(60\)90013-2](https://doi.org/10.1016/0022-5096(60)90013-2)
- Franke B, Quenneville P (2011) Numerical modeling of the failure behavior of dowel connections in wood. *J Eng Mech* 137(3):186–195. [https://doi.org/10.1061/\(ASCE\)EM.1943-7889.0000217](https://doi.org/10.1061/(ASCE)EM.1943-7889.0000217)
- Franke B, Quenneville P (2014) Analysis of the fracture behavior of radiata pine timber and laminated veneer lumber. *Eng Fract Mech* 116:1–12. <https://doi.org/10.1016/j.engfracmech.2013.12.004>
- Frühmann K (2002) Fracture of wood on different hierarchical levels [Doctoral dissertation, Technische Universität Wien]
- Frühmann K, Reiterer A, Tschegg EK, Stanzl-Tschegg SS (2002) Fracture characteristics of wood under mode I, mode II and mode III loading. *Philos Mag A* 82(17–18):3289–3298. <https://doi.org/10.1080/01418610208240441>
- Gilbert BP, Dias-da-Costa D, Lebée A, Foret G (2020) Veneer-based timber circular hollow section beams: Behaviour, modelling and design. *Constr Build Mater* 258:120380. <https://doi.org/10.1016/j.conbuildmat.2020.120380>
- Gilbert BP, Fernando D, Pham CH (2022) Experimental techniques in structural testing: common mistakes, how to avoid them and other advice. *Structures* 41:1687–1699. <https://doi.org/10.1016/j.istruc.2022.05.091>
- Guitard D (1987) *Mécanique du matériau bois et composites (Mechanics of wood and composite materials).* Cepadues Éditions, France
- Gustafsson PJ (1988) A study of strength of notched beams. Paper presented at the Proceedings of 21st Meeting of CIB-W18, Parksville, Canada
- International Council for Building Research (1989) Working Commission W18A—Timber structures CIB-W18A, meeting
- Jensen JL, Nakatani M, Quenneville P, Walford B (2011) A simple unified model for withdrawal of lag screws and glued-in rods. *Eur J Wood Prod* 69(4):537–544. <https://doi.org/10.1007/s00107-010-0478-y>
- Jones DL, Chisholm D (1975) An investigation of the edge-sliding mode in fracture mechanics. *Eng Fract Mech* 7(2):261–270. [https://doi.org/10.1016/0013-7944\(75\)90007-7](https://doi.org/10.1016/0013-7944(75)90007-7)
- Kachanov L (1986) Introduction to continuum damage mechanics, vol 10. Springer Science and Business Media, Berlin
- Komatsu K, Sasaki H, Maku T (1974) Evaluation of fracture toughness for wood-epoxy adhesive system under external shear force, vol 57. *Bulletin of the Wood Research Institute Kyoto University, Kyoto*
- Larsen H, Gustafsson P (1991) The fracture energy of wood in tension perpendicular to the grain. Errata, and annex A12 and A13 to CIB paper W18A/23-19-2. Results from a joint testing project. Paper presented at the Proceedings of CIB W18 meeting 24. Princes Risborough, United Kingdom. CIB-W18A/24-19-1
- Leggate W, McGavin RL, Miao C, Outhwaite A, Chandra K, Dorries J, Knackstedt M (2020) The influence of mechanical surface preparation methods on southern pine and spotted gum wood properties: wettability and permeability. *BioResources* 15(4):8554. <https://doi.org/10.15376/biores.15.4.8554-8576>
- Leggate W, McGavin RL, Outhwaite A, Dorries J, Robinson R, Kumar C, Knackstedt M (2021a) The influence of mechanical surface preparation method, adhesive type, and curing temperature on the bonding of Darwin stringybark. *BioResources*. <https://doi.org/10.15376/biores.16.1.302-323>
- Leggate W, McGavin RL, Outhwaite A, Kumar C, Faircloth A, Knackstedt M (2021b) Influence of mechanical surface preparation methods on the bonding of southern pine and spotted gum: Tensile shear strength of lap joints. *BioResources* 16(1):46–61. <https://doi.org/10.15376/biores.16.1.46-61>
- Leggate W, Outhwaite A, McGavin RL, Gilbert BP, Gunalan S (2022) The effects of the addition of surfactants and the machining method on the adhesive bond quality of spotted gum glue-laminated beams. *BioResources* 17(2):3413–3434. <https://doi.org/10.15376/biores.17.2.3413-3434>
- Leka Y (2022) Determining key mechanical properties for connection design of softwood and hardwood sawn timber at various strain rates [Master of Engineering Thesis, Griffith University]. (Available by request to the second author of this paper)
- Ostapska K, Malo KA (2020) Wedge splitting test of wood for fracture parameters estimation of Norway spruce. *Eng Fract Mech* 232:107024. <https://doi.org/10.1016/j.engfracmech.2020.107024>
- Prokopski G (1995) Investigation of wood fracture toughness using Mode II fracture (shearing). *J Mater Sci* 30(18):4745–4750. <https://doi.org/10.1007/BF01153088>
- Queensland Government Department of Agriculture and Fisheries (2016) Queensland forest and timber industry: an overview. Technical report. Available at: <https://www.publications.qld.gov.au/dataset/f49c9111-4490-4fcc-947b-a490f6389c6b/resource/f01947e3-50bc-44ac-996e-e747fa02b00a/download/5288qldfor-estandtimberindustryoverview.pdf>
- Raftery GM, Whelan C (2014) Low-grade glued laminated timber beams reinforced using improved arrangements of bonded-in GFRP rods. *Constr Build Mater* 52:209–220. <https://doi.org/10.1016/j.conbuildmat.2013.11.044>
- Redman A (2017) Modelling of vacuum drying of Australian hardwood species [Doctoral dissertation, Queensland University of Technology]
- Reiner J, Wood J, Subhani M (2022) Mode II fracture of wood: comparison between end-notched flexure and compact shear testing. *Eng Fract Mech* 270:108561. <https://doi.org/10.1016/j.engfracmech.2022.108561>
- Reiterer A, Tschegg S (2002) The influence of moisture content on the mode I fracture behaviour of sprucewood. *J Mater Sci* 37(20):4487–4491. <https://doi.org/10.1023/A:1020610231862>
- Reiterer A, Stanzl-Tschegg S, Tschegg E (2000) Mode I fracture and acoustic emission of softwood and hardwood. *Wood Sci Technol* 34(5):417–430. <https://doi.org/10.1007/s002260000056>
- Richard H, Benitz K (1983) A loading device for the creation of mixed mode in fracture mechanics. *Int J Fract* 22(2):R55–R58. <https://doi.org/10.1007/BF00942726>
- Ross RJ (2010) *Wood handbook: Wood as an engineering material.* United States Department of Agriculture, Forest Service, Forest Products Laboratory, Madison, US

- Rug W, Badstube M, Schone W (1990) Determination of fracture energy of wood for tension perpendicular to grain. In: Proceedings of the international council for building research studies and documentation working commission W18A - timber structures CIB-W18A/23-19-1. Portugal, Lisbon, pp 459–493
- Sandhaas C (2012) Mechanical behaviour of timber joints with slotted-in steel plates [Doctoral thesis, Universität Karlsruhe]
- Vella R, Heitzmann MT, Redman A, Bailleres H (2019) Comparison of test methods for the determination of delamination in glued laminated timber. *BioResources* 14(4):7920–7934. <https://doi.org/10.15376/biores.14.4.7920-7934>
- Williams J, Birch M (1976) Mixed mode fracture in anisotropic media. *Cracks and Fract* 601(1):125–137
- Wu E (1967) Application of fracture mechanics to anisotropic plates. *J Appl Mech* 34(4):967–974. <https://doi.org/10.1115/1.3607864>
- Yoshihara H (2008) Mode II fracture mechanics properties of wood measured by the asymmetric four-point bending test using a single-edge-notched specimen. *Eng Fract Mech* 75(16):4727–4739. <https://doi.org/10.1016/j.engfracmech.2008.06.010>

Publisher's Note Springer Nature remains neutral with regard to jurisdictional claims in published maps and institutional affiliations.